Process Variation Sensitivity of Spin-Orbit Torque Perpendicular Nanomagnets in DBNs

Hossein Pourmeidani¹⁰, Punyashloka Debashis^{2,3}, Zhihong Chen¹⁰, and Ronald F. DeMara¹⁰

¹Department of Electrical and Computer Engineering, University of Central Florida, Orlando, FL 32816 USA

²School of Electrical and Computer Engineering, Purdue University, West Lafayette, IN 47907 USA

³Components Research, Intel Corporation, Hillsboro, OR 97124 USA

Neuromorphic architectures with low energy barrier nanomagnetic devices have been attracting increasing interest over the past few years. More recently, a low barrier nanomagnet (LBNM)-based probabilistic device (p-bit) has been shown to be the basis of neuronal nodes in deep belief networks (DBNs). The LBNMs with perpendicular magnetic anisotropy (PMA) are analyzed and optimized in the interest of achieving stochasticity present in the learning system. In p-bit-based DBNs, several defects, such as variation of the nanomagnet diameter (σd) , thickness (σt_f) , and anisotropy field (σH_K) , which results in alteration of the fluctuation speed of the p-bit's nanomagnet can impair functionality. In this article, the accuracy of p-bit-based DBNs is examined under variation of nanomagnet diameter, thickness, and anisotropy field for various tilt angles and temperatures. As evaluated for the MNIST data set for temperature and tilt angle of 300 K and 25°, accordingly, it is shown that the process variation (PV) of σd , σt_f , and σH_K can be tolerated up to 8%, 23%, and 25%, respectively. A new method is developed to control the fluctuation frequency of the output of a p-bit device by employing a feedback mechanism. The feedback can alleviate this PV sensitivity of p-bit-based DBNs. The compact and low complexity method, which is presented by introducing the self-compensating circuit, can alleviate the influences of PV in fabrication and practical implementation.

Index Terms—Deep belief network (DBN), low barrier nanomagnetic (LBNM) devices, probabilistic spin logic device (p-bit).

I. INTRODUCTION AND BACKGROUND

GROWING focus of recent research has been on gaining the advantages of binary stochastic neurons as the basis of brain-inspired computing frameworks. By considering the widespread utilization of stochasticity in the neuromorphic science field, inadequate focus has been on hardware implementation of stochastic computing models. The underlying CMOS hardware employed in several approaches to realizing the neuronal functionality needs area-consuming pseudo or true random number generators to perform stochastic behavior due to its deterministic behavior. In contrast, inherent randomness is demonstrated in post-CMOS technologies, such as spintronic devices within their switching processes. In [4]–[13], efficient and small neuronal hardware in several learning systems is realized by utilizing these single-bit spin-based hardware units' stochasticity behavior.

The probabilistic spin logic device (p-bit) with perpendicular magnetic anisotropy (PMA) is among the new building block, which is completely tunable by spin-orbit torque (SOT) [1]–[3]. The output of p-bit can be varied by adjusting a dc current through the giant spin Hall effect (GSHE) Ta Hall bar, as shown in Fig. 1. By adjusting the direction of the dc current (I_C), then the magnetization direction will probabilistically favor either the "UP" or "DOWN" state that produces a sigmoidal curve by taking the average of the states as the current is swept across a range of values. The charge

Manuscript received February 10, 2021; accepted April 13, 2021. Date of publication April 23, 2021; date of current version June 23, 2021. Corresponding author: H. Pourmeidani (e-mail: hossein.pourmeidani@knights.ucf.edu).

Color versions of one or more figures in this article are available at https://doi.org/10.1109/TMAG.2021.3075391.

Digital Object Identifier 10.1109/TMAG.2021.3075391

current flowing through the layer with GSHE modifies the dwell time in the two stable states and, as a result, changes the output significantly for a low barrier nanomagnet (LBNM) with a thermal barrier close to zero kT. According to the thermal energy, the p-bit is implemented with a thermally stable nanomagnet in regular MRAM cells with a high energy barrier. As a result, the p-bit offers a thresholding behavior appropriate for neural network applications and meanwhile works in non-volatile storages in the form of a single-bit element. The magnetization direction in the device is read through anomalous Hall effect (AHE), which requires large CMOS circuitry to amplify the weak output signal generated. However, if the single nanomagnet of the device can be replaced by an MTJ where the free layer is designed to have a similarly weak perpendicular anisotropy, then the magnetization fluctuations can be read through a much stronger tunneling magnetoresistance (TMR) effect. A similar device is proposed in [7] and shown in Fig. 1. This device uses the same technology as the SOT-MRAM, with one modification, i.e., the MTJ free layer is made thermally unstable. Hence, the implementation of p-bits requires small changes to the MRAM fabrication flow. In [5]-[12], the utilization of thermally unstable low energy barrier p-bits on the basis of superparamagnetic materials has been examined theoretically and experimentally in order to achieve probabilistic neuromorphic paradigms by utilizing functional spintronic devices. As an illustration, the work of [13] and [14] employed them in spiking neural networks (SNNs), while the work of [15] and [16] investigated deep belief network (DBN) structures by employing p-bit devices. In this article, we have carried out several simulations to explore the effects of process variation (PV), including anisotropy field, nanomagnet thickness, and

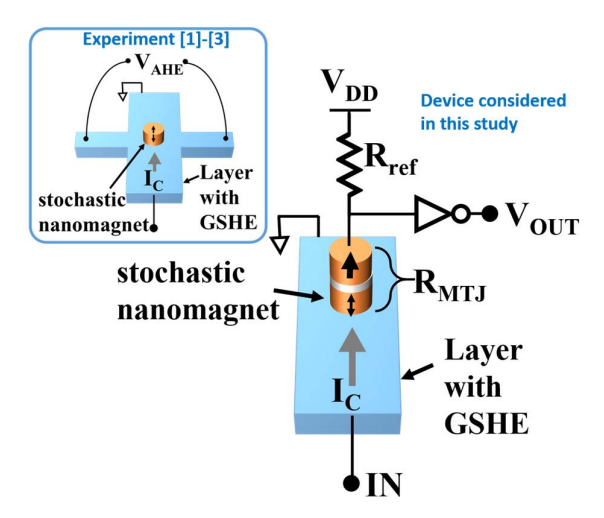


Fig. 1. Diagram of the probabilistic device (p-bit) with perpendicular magnetic anisotropy (PMA) as a binary stochastic neuron for DBNs [1]–[3]. The experiments in [1]–[3] used AHE to read the magnetization state. This read scheme can be replaced by an MTJ. The magnetization state of the weak perpendicular anisotropy free layer can be read through the resistance change of an MTJ as proposed in [7].

nanomagnet diameter on the p-bit devices' energy barrier and their resulting influence on the proposed DBN architecture's accuracy. Measurements and analysis results indicate that p-bit-based DBNs are sensitive more to diameter, anisotropy field, and then thickness. Thus, here, we introduce an in-circuit design approach to self-compensate for PV LBNM SOT-based devices.

II. P-BIT AS A STOCHASTIC NEURON

A thermally unstable low energy barrier SOT-MRAM device with a PMA nanomagnet $(E_b \sim 18 k_B T)$ is proposed by Debashis et al. [1]-[3]. By configuring the nanomagnet's energy barrier to be equivalent or less than the ambient thermal noise, the nanomagnet will act in the form of a true random number generator (TRNG) and randomly fluctuate among "UP" and "DOWN" states. The p-bit has the ability to work as a tunable TRNG by tuning the probability of nanomagnet being in one of the two states through an external input. A three-terminal SOT-based neuron is much more suitable to be utilized into neural networks for several reasons. The shared read/write path across the whole device in STT-based neurons results in a read reliability issue, while serious stress can be applied on the MTJ by the write current. Also, the shared read and write path causes the concatenation of these devices into a neural network to become complicated since the input and output signals are not isolated from each other. Moreover, due to considerable incubation delays of STT-MRAM devices, they are unable to work reliably at ns and sub-ns scales [17]-[20]. The functionality of this device is formulated through the MTJ conductance [14]

$$G_{\text{MTJ}} = G_0 \left[1 + m_z \frac{\text{TMR}}{2 + \text{TMR}} \right] \tag{1}$$

where the MTJ conductance's average $(G_P+G_{AP})/2$ is G_0, m_z is the free-layer magnetization, and the ratio of tunneling magnetoresistance is TMR. By substituting TMR = $(G_P/G_{AP})-1$,

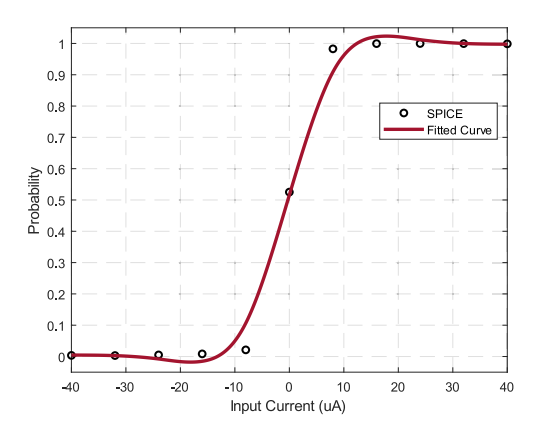


Fig. 2. Probability output of SOT-MRAM-based neuron being in logic state "1" versus its input current over input range from -40 to $40~\mu A$.

it can be deduced from (1) that $G_{\rm MTJ} = G_P$ and $G_{\rm MTJ} = G_{\rm AP}$, when $m_Z = +1$ and $m_Z = -1$, respectively. Considering $m_Z = +1$, we have

$$G_{\text{MTJ}} = \frac{G_P + G_{\text{AP}}}{2} \left[1 + \frac{(G_P/G_{\text{AP}} - 1)}{(G_P/G_{\text{AP}} + 1)} \right] = G_P.$$
 (2)

Similarly, substituting $m_Z = -1$, we have

$$G_{\text{MTJ}} = \frac{G_P + G_{\text{AP}}}{2} \left[1 - \frac{(G_P/G_{\text{AP}} - 1)}{(G_P/G_{\text{AP}} + 1)} \right] = G_{\text{AP}}.$$
 (3)

The fluctuations in the MTJ conductance are converted to a voltage at the input of the inverter through the potential divider formed by the MTJ and the reference resistance R_{ref} (see Fig. 1)

$$V_M/V_{\rm DD} = \pm \frac{R_{\rm MTJ} - R_{\rm ref}}{R_{\rm MTJ} + R_{\rm ref}} \tag{4}$$

where V_M is the voltage at the input of the inverter, $R_{\rm MTJ} = (1/G_{\rm MTJ})$ is the fluctuating MTJ resistance, and $R_{\rm ref}$ is the reference resistance.

The p-bit device utilizes a near-zero energy barrier circular nanomagnet without shape anisotropy. The magnetization of free layer for the MTJ conductance discussed in (1) is given by the stochastic Landau–Lifshitz–Gilbert (LLG) [7]

$$(1 + \alpha^{2})d\hat{m}/dt$$

$$= -|\gamma|\hat{m} \times \vec{H} - \alpha|\gamma|(\hat{m} \times \hat{m} \times \vec{H})$$

$$+ 1/qN(\hat{m} \times \vec{I}_{s} \times \hat{m}) + (\alpha/qN(\hat{m} \times \vec{I}_{s}))$$
 (5)

where the nanomagnet damping coefficient is α , the electron charge is q, the electron gyromagnetic ratio is γ , and \overline{I}_S is the free-layer spin current incident. Fig. 2 shows the relation among input current and the probability of output being in state "1." As shown, approximately 50% probability of p-bit's output being in state "1" is obtained when input current equals 0 μ A. Thus, besides being compact with low area requirement, it provides a tunable probability of generating a "0" or "1" output state-based on the input current.

Stochastic circuits play a significant role in the implementation of networks with probabilistic nodes. For instance, learning networks employing p-bits are worthwhile in realizing DBNs in a way that a learning algorithm in software trains

weights offline and inference tasks is effectively performed repeatedly by utilizing the hardware. Unstable low barrier nanomagnets present a direct mechanism to realize stochastic sigmoidal neurons in DBNs through leveraging the arbitrarily fluctuating magnetization to produce a stochastic time-varying output voltage. If these nanomagnets are designed to have as low energy barriers as feasible, then many random outputs are produced in a short period of time. Under this strategy, a low energy barrier ($E_b \ll 40~k_BT$) PMA nanomagnet has the capability of flipping back and forth, which can be tuned by modulating the input current.

III. EFFECTS OF PV ON P-BIT

Although the p-bit device is more error tolerant than conventional digital computing devices, it is still not completely tolerant of device-to-device variations and defects [22]. It is shown that the delocalized and localized defects impact the power spectral density [23]. The power spectral density is impacted much more by delocalized defects than localized defects suchlike thickness variations, whereas it is quite indifferent to the presence of moderate barrier height change and small localized defects [24]–[26]. The magnetization's fluctuation rate in low barrier nanomagnets is altered substantially by delocalized defects. Consequently, p-bit-based neurons' applications for neuromorphic architectures will be impacted by considering the necessity of the fluctuation rate in stochastic computing applications.

As stated in the following equation, through decreasing the total magnetic moment by managing a small anisotropy field (H_K) and/or reducing volume (V), the near-zero energy barrier in p-bit devices is attainable [27]

$$E_B = \frac{1}{2} H_K M_s V = \frac{1}{2} H_K M_s (\pi (d/2)^2 t_f)$$
 (6)

where the thickness and diameter of the PMA nanomagnet are t_f and d, respectively. P-bits may demonstrate different "as-built" energy barriers as a consequence of the fabrication PVs of low energy barrier nanomagnets [22]. In accordance with (6), variations in nanomagnet thickness (σt_f) and anisotropy field (σH_K) cause linear variations in energy barrier (σE_B). However, variations in nanomagnet diameter (σd) cause quadratic variations in energy barrier (σE_B).

As noted in the prior section, the low energy barrier nanomagnet will oscillate irregularly between the "UP" and "DOWN" states. The dwell time of magnetization in the "UP" and "DOWN" states generates a distribution, which affirms the stochastic fluctuation of nanomagnet. A sigmoidal distribution is discovered over a series of samples by oscillating the PMA nanomagnet's magnetization direction between "UP" and "DOWN" states. Thermal energy instigates these state Transitions, which is sufficient to arbitrarily fluctuate as long as adequately small energy barrier is used. The nanomagnet's fluctuation speed can be attained from the average dwell time in "UP" and "DOWN" states $\tau_{\rm Up}$ and $\tau_{\rm Down}$ as follows [1], [3], [28]:

$$\tau^{-1} = (\tau_{\text{Up}} \times \tau_{\text{Down}})^{1/2} \tag{7}$$

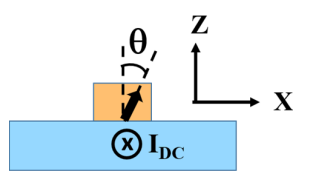


Fig. 3. Tunability of the average magnetization component in the Z-direction, while the magnetization lies in the ZX plane.

and the dependence of this time scale on the nanomagnet energy barrier (E_B) is consistent with the Arrhenius-like law [29]

$$\tau = \tau_0 \times \exp(E_B/K_BT) \tag{8}$$

where the average dwell time of the magnetization is τ , the energy barrier separating the two stable states is E_B , the Boltzmann constant is k_B , and the temperature is T. τ_0 is a material parameter, often referred to as the attempt time and is reported to be around $10 \text{ ps}^{-1} \text{ ns}^1$. From this equation, it can be seen that when the thermal energy (k_BT) is comparable to E_B , the magnetization fluctuates at a rate given by $1/\tau$, which can reach upward of 1 GHz. Thereby, the probabilistic behavior of the p-bit devices will be affected by decreasing or increasing the fluctuation speed of nanomagnet through increasing or reducing the energy barrier, respectively.

In a low perpendicular anisotropy p-bit device, any little in-plane anisotropy can result in a considerable tilt angle (θ) that may not be detectable in high perpendicular anisotropy magnets. The in-plane spins do not impact the desired direction of the average magnetization component in the Z-direction when there is no tilt in the magnet's anisotropy. As a result, the average magnetization component in the Z-direction remains around zero. Accordingly, the tilt direction is toward the X-axis in the ZX-plane, as shown in Fig. 3. It has been proved that, in the Z-direction, perfect tunability of the average magnetization component can be attained for tilt angles around 25° [1]–[3].

The fabrication imperfections have a substantial impact on the performance and accuracy of neuromorphic applications. Accordingly, these imperfections cause several defects, which are needed to be tolerated for p-bit-based neurons in DBNs. In general, there are two solutions for these problems caused by variations: 1) refine materials and production processes in a fabrication-oriented approach and 2) solve the aforementioned PV challenges in a circuit-level approach. Here, a variation analysis will be carried out to report the satisfactory range of production process and tolerances for crucial parameters affecting the p-bit devices in terms of energy barrier and accuracy. In this study, we use a variation-less $784 \times 200 \times$ 10 DBN circuit as the baseline to investigate the accuracy of p-bit-based DBNs, as shown in Fig. 4. The probabilistic inference network simulator (PIN-Sim) [16] is employed as a circuit-level implementation of DBNs. In PIN-Sim, embedded MRAM-based p-bit neurons and resistive crossbars are utilized as activation functions and weighted connections, respectively. Here, the accuracy of DBN is calculated as the number of input images that are correctly predicted divided by all the

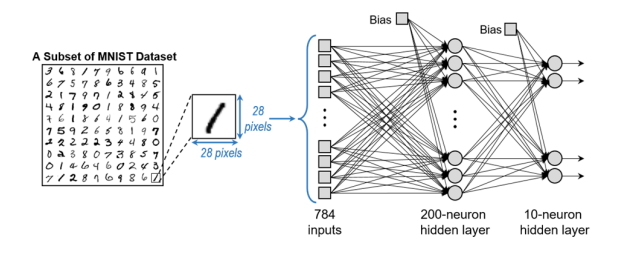


Fig. 4. Employed simulation framework including a $784 \times 200 \times 10$ DBN implemented for MNIST pattern recognition application and a subset of MNIST data set, where the output neurons indicate to digital output class.

predictions as follows [30]:

$$Accuracy = \frac{Number of Correct Predicted Images}{Total Number of Predictions}.$$
 (9)

More specifically, a correct prediction is considered as a true positive or true negative, which is an input image that the DBN correctly predicted as true or false, respectively. Therefore, the total number of predictions is defined as the sum of correct predictions involving true positives and true negatives and incorrect predictions, including false positives and false negatives as follows [30]:

$$Accuracy = \frac{TN + TP}{TN + TP + FN + FP}$$
 (10)

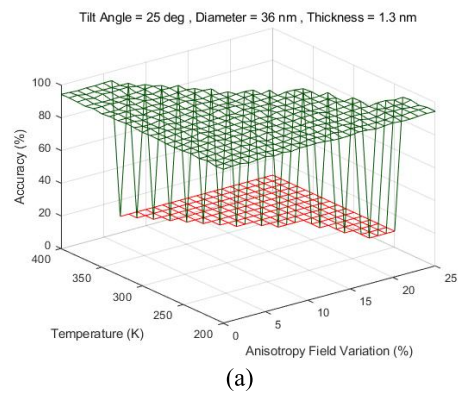
where TN is true negatives, TP denotes true positives, FN represents false negatives, and FP is false positives.

IV. PV ANALYSIS OF P-BIT-BASED DBN

In this section, the impact of PV on the p-bit-based DBN is evaluated. We have modeled a random variation distribution of three types of PV, which affects the fluctuation speed of nanomagnet: 1) (σH_K) : variations in the anisotropy field (H_K) ; 2) (σd) : variations in the diameter (d) of nanomagnet; and 3) (σt_f) : variations in the thickness (t_f) of nanomagnet, for various temperatures and tilt angles (θ) . The nanomagnet parameters used in our simulation for a variation-less p-bit-based DBN as the baseline are $H_K = 400$ mT, D = 36 nm, $t_f = 1.3$ nm, $\theta = 25^\circ$, and temperature = 300 K. The lower and higher energy barriers are realized by decreasing and increasing these three parameters. As described in (7) and (8), reducing and increasing the energy barrier increases and reduces the nanomagnet's probabilistic fluctuation speed in SOT-MRAM devices.

A. Individual Variation

In this section, we analyze the impact of individual parameter variation, while temperature and tilt angle are varying for specified ranges. The results are achieved by MATLAB simulation for MNIST handwritten digit recognition application by utilizing $60\,000$ training images on a $784\times200\times10$ DBN. It is mentioned that variations in the PIN-Sim framework are applied by utilizing a randomly generated parameters value between the baseline value of each parameter and a maximum parameter variation of 25%.



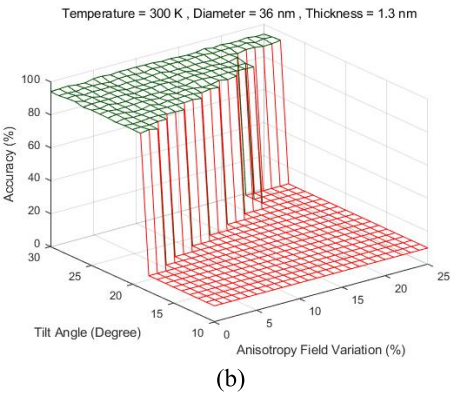


Fig. 5. Accuracy of p-bit-based DBN versus σH_M for (a) temperature of 200–400 K and (b) tilt angles of 10° – 30° .

1) Anisotropy Field Variation: Fig. 5(a) and (b) shows the accuracy of p-bit-based DBN versus σH_K for various temperatures of 200-400 K and tilt angles of 10°-30°, respectively. Other nanomagnet parameters are the same as the baseline and fixed. As shown in Fig. 5(a), anisotropy field variations do not affect the accuracy of p-bit-based DBN, while temperature values range from 200 to 250 K. The worst case scenario is when temperature = 400 K in the presence of around 7% PV in anisotropy field in which the accuracy will be reduced to an unsuitable value of around 10% (i.e., error rate around 90%). As it can be seen in Fig. 5(b), tilt angle should be at least around 18°, while PV in anisotropy field can be completely tolerated up to 25% (i.e., $\sigma H_K = 25\%$) for at least a tilt angle of 28°. Thus, the PV of anisotropy field in p-bit-based DBNs is seen to be tolerated up to around 20% for the baseline values of temperature and tilt angle. In this case, for the temperature of 300 K and tilt angle 25°, baseline values are used throughout.

2) Diameter Variation: The accuracy of p-bit-based DBN versus σd for various temperatures of 200–400 K and tilt angles of 10° – 30° is shown in Fig. 6(a) and (b), respectively, whereas other nanomagnet parameters are equivalent to the baseline values and fixed. By decreasing temperature, higher diameter variation can be tolerated, as shown in Fig. 6(a). The best case scenario is when temperature = 250 K in the presence of around 14% PV in diameter in which the accuracy of around 90% is still obtained. As can be observed in Fig. 6(b), diameter variation can be tolerated

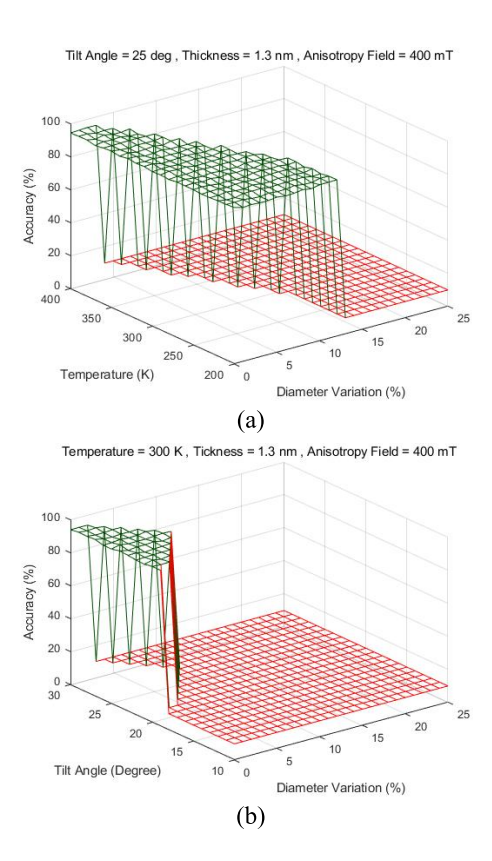


Fig. 6. Accuracy of p-bit-based DBN versus σd for (a) temperature of 200–400 K and (b) tilt angles of 10° – 30° .

up to around 8%, i.e., $\sigma d = 8\%$, for a small range of tilt angles. Hence, the process variation of diameter in p-bit-based DBNs is witnessed to be tolerated up to around 8% for the baseline values of temperature and tilt angle. In comparison to anisotropy field variation, p-bit-based DBNs are more sensitive to diameter variation.

3) Thickness Variation: Fig. 7(a) and (b) shows the accuracy of p-bit-based DBN versus σt_f , while temperature and tilt angle range from 200 to 400 K and 10° to 30°, respectively. Other nanomagnet parameters are fixed values that are equivalent to the baseline values. Thickness variations do not impact the accuracy of p-bit-based DBN, while temperature values range from 200 to 220 K, as shown in Fig. 7(a). The least thickness variation tolerance is achieved when temperature = 400 K in the presence of around 8% PV in thickness in which the accuracy will be reduced to an inappropriate value of around 10% (i.e., error rate around 90%). As shown in Fig. 7(b), tilt angle should be at least around 18°, while process variation in thickness completely can be tolerated up to 25% (i.e., $\sigma t_f = 25\%$) for at least a tilt angle of 28°. Therefore, the PV of thickness in p-bit-based DBNs is seen to be tolerated up to around 23% for the baseline values of temperature and tilt angle. The p-bit-based DBNs are less sensitive to thickness variation in relation to anisotropy field and diameter variations.

B. Impact of Multiple Sources of Variation

In this section, we analyze the impact of multiple variation sources of σH_K , σd , and σt_f ranging from 0% to 25%

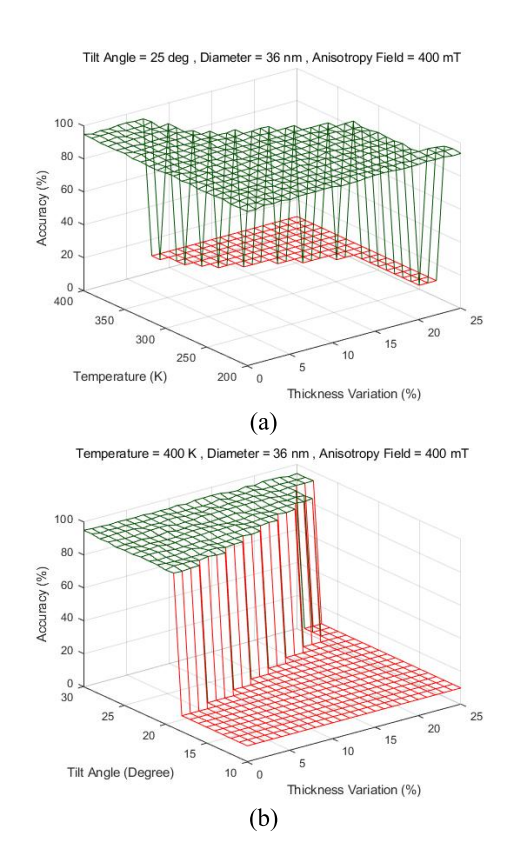


Fig. 7. Accuracy of p-bit-based DBN versus σt_f for (a) temperature of 200–400 K and (b) tilt angles of 10° – 30° .

on the p-bit-based DBNs, while temperature and tilt angle are fixed values that are equivalent to the baseline values of 300 K and 25°, respectively. The results are achieved by the MATLAB simulation for MNIST handwritten digit recognition application by utilizing 60 000 training images on a $784 \times 200 \times 10$ DBN. As previously mentioned, the maximum value of variation of all parameters is limited to 25%.

Fig. 8(a)-(c) shows the accuracy of p-bit-based DBN for three different combinations of σH_K , σd , and σt_f , respectively. As we can see, by increasing variation in a parameter, less variation in another parameter is tolerable. Thus, the highest variation tolerance for each parameter is obtained when variation in other parameters is 0% (i.e., other parameters are set to the baseline values). In other words, less variation in each parameter is tolerable in the presence of variation in more than one parameter compared to the scenarios that only one parameter has variation. As shown in Fig. 8(a), the highest multiple variation tolerance for a combination of σd and σH_K is obtained when $\sigma d = 5\%$ and $\sigma H_K = 7\%$, which results in an aggregated variation of 12%. Fig. 8(b) shows that the highest multiple variation tolerance for a combination of σt_f and σd is attained when $\sigma t_f = 15\%$ and $\sigma d = 5\%$, which leads to an aggregated variation of 20%. The highest multiple variation tolerance for a combination of σt_f and σH_K is achievable when $\sigma t_f = 11\%$ and $\sigma H_K = 7\%$, which results in an aggregated variation of 18%. The results show that the pbit-based DBNs are more sensitive to the multiple variations of $(\sigma d \text{ versus } \sigma H_K)$, $(\sigma t_f \text{ versus } \sigma H_K)$, and $(\sigma t_f \text{ versus } \sigma d)$. By employing a feedback approach, this knee effect factor

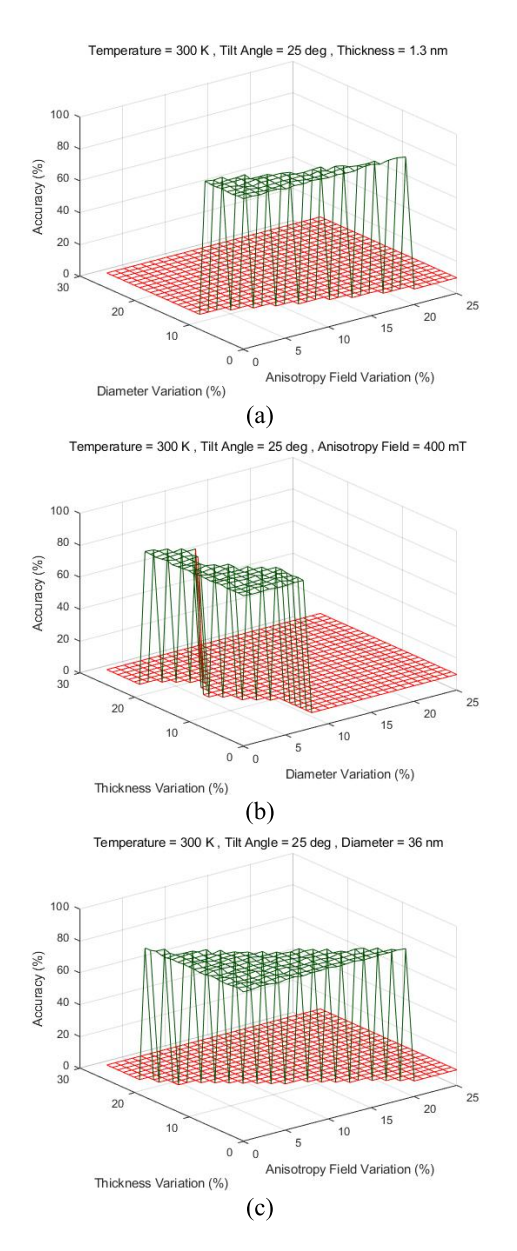


Fig. 8. Accuracy of p-bit-based DBN for (a) σd versus σH_K , (b) σt_f versus σd , and (c) σt_f versus σH_K .

can be mitigated in practice by changing the nanomagnet's fluctuation rate, as explained in Section V.

V. P-BIT WITH FEEDBACK

In this section, we present a method to control the fluctuation frequency of the output of a p-bit. In this device, the output voltage tracks the magnetization direction through the anomalous Hall effect and fluctuates randomly between two values, "UP" and "DOWN." The energy barrier of the nanomagnet defines the average fluctuation frequency (f_0) through the following equation:

$$f_0 = \left(\tau_0 \exp\left(\frac{E_B}{k_B T}\right)\right)^{-1}.\tag{11}$$

A dc current through the layer with GSHE biases the stochastic output of the device toward one of the two states. However,

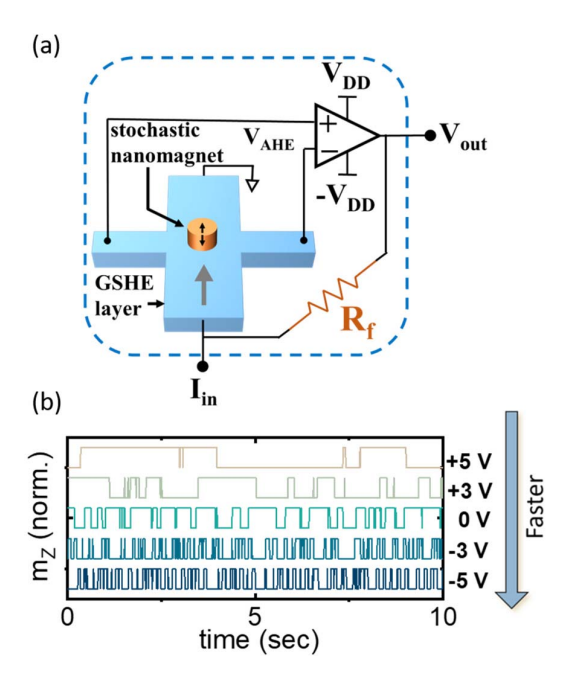


Fig. 9. Tuning the effective energy barrier through electrical feedback. (a) Measurement configuration with the feedback implemented through a simple resistor of value 360 K Ω . (b) Measurement of the output fluctuations of the device for various feedback configurations.

instead of a dc current, when the device's output is amplified and fed back to the layer with GSHE, the fluctuation of the magnetization based on the strength and polarity of the feedback gets slower or faster, analogous to temperature annealing. Fig. 9(a) shows the device schematic with the feedback configuration. The value of the resistor R_f controls the feedback, which alters the feedback current flowing through the layer with GSHE. However, for experimental simplicity, the resistor value is kept fixed and V_{DD} of the amplifier is changed in both magnitude and sign. Fig. 9(b) shows the experimentally measured stochastic signal at the output of this device for different feedback configurations. A large positive V_{DD} corresponds to a strong positive feedback, whereas a large negative $V_{\rm DD}$ corresponds to a strong negative feedback. It can be seen that the fluctuations at the device output become progressively faster as the feedback changes from positive to negative (amplifier $V_{\rm DD}$ changing from +5 to -5 V). The output signals for various feedback configurations are shifted artificially along the vertical axis for clarity. Please note that in this experiment, the average fluctuation time scale, t, is 144 ms at no feedback. This slow fluctuation speed is due to the fact that the nanomagnet used in this experiment had an energy barrier, $E_B = 18 k_B T$. In order to achieve fluctuations of 1 ns, this energy barrier can be reduced to be closer to $1 k_B T$ by two approaches.

 By designing weaker perpendicular anisotropy stacks through the ferromagnetic layer thickness optimization, in a CoFeB/MgO perpendicular anisotropy magnetic stack, the effective anisotropy energy density is given by [31]

$$\frac{1}{2}M_sH_K = K_{\text{eff}} = \frac{K_i}{t_F} - \frac{M_S^2}{2\mu_0}$$
 (12)

where K_i is the interface anisotropy, t_F is the thickness of the ferromagnetic layer, M_S is the saturation magnetization, and μ_0 is permeability of free space. It can be seen from the above equation that by engineering t_F to make the RHS close to zero, we can make the effective perpendicular anisotropy to vanish, hence resulting in very low E_B .

2) By fabricating magnets with smaller diameters through advanced lithography, the volume, and hence E_B , of the nanomagnet can be made smaller. With currently available industrial lithographic technology, a diameter of 30 nm is possible [32].

In this device, a charge current input to the heavy metal electrode adjacent to the nanomagnet produces a torque on its magnetization via SOT. This was heuristically explained as a tilting of the energy landscape, where a positive current tilts the energy landscape toward the "UP" state and a negative current causes a tilt toward the "DOWN" state. When the device output is converted into a charge current and fed back to the device input, the tilt of the energy landscape dynamically depends on the instantaneous state of magnetization. This results in a dynamic modification of the effective energy barrier. The case for the negative feedback case is described as follows. When the magnetization is in the "UP" state, the negative feedback produces a negative charge current through the input that tilts energy landscape toward the "DOWN" state, thus reducing energy barrier to hop out of the "UP" state. Likewise, once the magnetization is in the "DOWN" state, a positive feedback current is produced at the input that tilts the energy landscape toward the "UP" state, hence reducing energy barrier to hop out of the "DOWN" state. Hence, a negative feedback results is an overall reduction of the effective energy barrier to switch to the other state. Following the modified Neel-Brown model [33], [34] to include the effect of spin torque on the nanomagnet due to the current flowing through the layer with GSHE, we have the following expression for the fluctuation frequency:

$$f_0 = \left(\tau_0 \exp\left(\frac{E_{B,\text{eff}}}{k_B T}\right)\right)^{-1} \tag{13}$$

where the effective energy barrier ($E_{B,eff}$) is given by

$$E_{B,\text{eff}} = E_B \left(1 \pm \frac{I_{\text{feedback}}}{I_C} \right) \tag{14}$$

where the nanomagnet's intrinsic energy barrier is E_B given in (6), the feedback current is I_{feedback} , and the critical current for magnetization switching at zero temperature is I_C . This results in a faster fluctuation rate, as seen by replacing E_B with a smaller $E_{B,\text{eff}}$ in (11). By considering the GSHE layer, resistance is much smaller than R_f , and I_{feedback} can be defined as V_{DD}/R_f . Then, by replacing V_{DD}/I_C with R_0 , the below expression is obtained for the magnet's effective energy barrier

$$E_{B,\text{eff}} = E_B \left(1 \pm \frac{R_0}{R_f} \right). \tag{15}$$

From (13) and (15), it is clearly seen that the p-bit's fluctuation frequency can be managed by altering the feedback resistor, as is proved in the experiment.

VI. CONCLUSION

Here, we explored an approach to alleviate the PV's impact on the p-bit's energy barrier and their following effect on the accuracy of p-bit-based DBNs. In the proposed technique, it was demonstrated that a variation in the parameters of nanomagnet diameter (σd) , thickness (σt_f) , and anisotropy field (σH_K) leads to variation in the nanomagnet's fluctuation speed of the p-bit's devices. As evaluated for the MNIST data set for temperature and tilt angle of 300 K and 25°, accordingly, it is shown that the PV of σd , σt_f , and σH_K can be tolerated up to 8%, 23%, and 25%, respectively. It implies that in order to obtain the sigmoidal curve in the p-bit-based neuron, a mechanism is needed to control the nanomagnet's fluctuation speed. In this article, a variation tolerance technique is proposed by configuring p-bit with electrical feedback, which could considerably change the PMA nanomagnet's probabilistic fluctuation speed. In such a case, the device's output is amplified and fed back to the layer with GSHE, and based on the polarity and strength of the feedback, the fluctuation of magnetization gets slower or faster, which successfully compensates for the variation impacts.

ACKNOWLEDGMENT

This work was supported in part by the Center for Probabilistic Spin Logic for Low-Energy Boolean and Non-Boolean Computing (CAPSL), one of the Nanoelectronic Computing Research (nCORE) Centers as task 2759.006, a Semiconductor Research Corporation (SRC) Program sponsored by the National Science Foundation (NSF) under Grant CCF 1739635.

REFERENCES

- P. Debashis and Z. Chen, "Tunable random number generation using single superparamagnet with perpendicular magnetic anisotropy," in Proc. 76th Device Res. Conf. (DRC), Jun. 2018, pp. 1–2.
- [2] P. Debashis, P. Upadhyaya, and Z. Chen, "Electrical annealing and stochastic resonance in low barrier perpendicular nanomagnets for oscillatory neural networks," in *Proc. Device Res. Conf. (DRC)*, Jun. 2019, pp. 87–88.
- [3] P. Debashis, R. Faria, K. Y. Camsari, S. Datta, and Z. Chen, "Correlated fluctuations in spin orbit torque coupled perpendicular nanomagnets," *Phys. Rev. B, Condens. Matter*, vol. 101, no. 9, Mar. 2020, Art. no. 094405.
- [4] W. H. Choi et al., "A magnetic tunnel junction based true random number generator with conditional perturb and real-time output probability tracking," in *IEDM Tech. Dig.*, Dec. 2014, pp. 5–12.
- [5] B. Sutton, K. Y. Camsari, B. Behin-Aein, and S. Datta, "Intrinsic optimization using stochastic nanomagnets," *Sci. Rep.*, vol. 7, no. 1, p. 44370, Jun. 2017.
- [6] P. Debashis, R. Faria, K. Y. Camsari, J. Appenzeller, S. Datta, and Z. Chen, "Experimental demonstration of nanomagnet networks as hardware for ising computing," in *IEDM Tech. Dig.*, Dec. 2016, pp. 34.3.1–34.3.4.
- [7] K. Y. Camsari, R. Faria, B. M. Sutton, and S. Datta, "Stochastic p-bits for invertible logic," *Phys. Rev. X*, vol. 7, no. 3, Jul. 2017, Art. no. 031014.
- [8] A. Sengupta, P. Panda, P. Wijesinghe, Y. Kim, and K. Roy, "Magnetic tunnel junction mimics stochastic cortical spiking neurons," *Sci. Rep.*, vol. 6, no. 1, p. 30039, Sep. 2016.
- [9] A. Sengupta, M. Parsa, B. Han, and K. Roy, "Probabilistic deep spiking neural systems enabled by magnetic tunnel junction," *IEEE Trans. Electron Devices*, vol. 63, no. 7, pp. 2963–2970, Jul. 2016.
- [10] B. Behin-Aein, V. Diep, and S. Datta, "A building block for hardware belief networks," Sci. Rep., vol. 6, no. 1, pp. 1–10, Sep. 2016.

- [11] V. Ostwal, P. Debashis, R. Faria, Z. Chen, and J. Appenzeller, "Spintorque devices with hard axis initialization as stochastic binary neurons," Sci. Rep., vol. 8, no. 1, p. 16689, Dec. 2018.
- [12] G. Srinivasan, A. Sengupta, and K. Roy, "Magnetic tunnel junction enabled all-spin stochastic spiking neural network," in *Proc. Design*, *Automat. Test Eur. Conf. Exhib. (DATE)*, Mar. 2017, pp. 530–535.
- [13] D. Zhang, L. Zeng, Y. Zhang, W. Zhao, and J. O. Klein, "Stochastic spintronic device based synapses and spiking neurons for neuromorphic computation," in *Proc. IEEE/ACM Int. Symp. Nanosc. Archit.* (NANOARCH), Jul. 2016, pp. 173–178.
- [14] K. Y. Camsari, S. Salahuddin, and S. Datta, "Implementing p-bits with embedded MTJ," *IEEE Electron Device Lett.*, vol. 38, no. 12, pp. 1767–1770, Dec. 2017.
- [15] H. Pourmeidani, S. Sheikhfaal, R. Zand, and R. F. DeMara, "Probabilistic interpolation recoder for energy-error-product efficient DBNs with p-bit devices," *IEEE Trans. Emerg. Topics Comput.*, early access, Jan. 9, 2020, doi: 10.1109/TETC.2020.2965079.
- [16] R. Zand, K. Y. Camsari, S. Datta, and R. F. Demara, "Composable probabilistic inference networks using MRAM-based stochastic neurons," ACM J. Emerg. Technol. Comput. Syst., vol. 15, no. 2, pp. 1–22, Jun. 2019.
- [17] K. Garello et al., "SOT-MRAM 300 mm integration for low power and ultrafast embedded memories," in Proc. IEEE Symp. VLSI Circuits, Jun. 2018, pp. 81–82.
- [18] T. Devolder et al., "Single-shot time-resolved measurements of nanosecond-scale spin-transfer induced switching: Stochastic versus deterministic aspects," *Phys. Rev. Lett.*, vol. 100, no. 5, Feb. 2008, Art. no. 057206.
- [19] I. M. Miron et al., "Perpendicular switching of a single ferromagnetic layer induced by in-plane current injection," *Nature*, vol. 476, no. 7359, pp. 189–193, Aug. 2011.
- [20] L. Liu, C.-F. Pai, Y. Li, H. W. Tseng, D. C. Ralph, and R. A. Buhrman, "Spin-torque switching with the giant spin Hall effect of tantalum," *Science*, vol. 336, no. 6081, pp. 555–558, May 2012.
- [21] P. Forn-Díaz, L. Lamata, E. Rico, J. Kono, and E. Solano, "Ultra-strong coupling regimes of light-matter interaction," *Rev. Modern Phys.*, vol. 91, no. 2, Jun. 2019, Art. no. 025005.
- [22] J. L. Drobitch and S. Bandyopadhyay, "Reliability and scalability of p-bits implemented with low energy barrier nanomagnets," *IEEE Magn. Lett.*, vol. 10, pp. 1–4, 2019.

- [23] M. A. Abeed and S. Bandyopadhyay, "Sensitivity of the power spectra of thermal magnetization fluctuations in low barrier nanomagnets proposed for stochastic computing to in-plane barrier height variations and structural defects," SPIN, vol. 10, no. 1, Mar. 2020, Art. no. 2050001.
- [24] M. A. Abeed and S. Bandyopadhyay, "Low energy barrier nanomagnet design for binary stochastic neurons: Design challenges for real nanomagnets with fabrication defects," *IEEE Magn. Lett.*, vol. 10, pp. 1–5, 2019.
- [25] J. Kaiser, A. Rustagi, K. Y. Camsari, J. Z. Sun, S. Datta, and P. Upadhyaya, "Subnanosecond fluctuations in low-barrier nanomagnets," *Phys. Rev. A, Gen. Phys.*, vol. 12, no. 5, Nov. 2019, Art. no. 054056.
- [26] O. Hassan, R. Faria, K. Y. Camsari, J. Z. Sun, and S. Datta, "Low-barrier magnet design for efficient hardware binary stochastic neurons," *IEEE Magn. Lett.*, vol. 10, pp. 1–5, 2019.
- [27] K. Y. Camsari, B. M. Sutton, and S. Datta, "P-bits for probabilistic spin logic," Appl. Phys. Rev., vol. 6, no. 1, Mar. 2019, Art. no. 011305.
- [28] D. Vodenicarevic et al., "Low-energy truly random number generation with superparamagnetic tunnel junctions for unconventional computing," Phys. Rev. A, Gen. Phys., vol. 8, no. 5, Nov. 2017, Art. no. 054045.
- [29] L. Lopez-Diaz, L. Torres, and E. Moro, "Transition from ferromagnetism to superparamagnetism on the nanosecond time scale," *Phys. Rev. B*, *Condens. Matter*, vol. 65, no. 22, May 2002, Art. no. 224406.
- [30] D. Chicco and G. Jurman, "The advantages of the Matthews correlation coefficient (MCC) over F1 score and accuracy in binary classification evaluation," *BMC Genomics*, vol. 21, no. 1, pp. 1–13, Dec. 2020.
- [31] S. Ikeda et al., "A perpendicular-anisotropy CoFeB-MgO magnetic tunnel junction," Nature Mater., vol. 9, no. 9, pp. 721–724, Jul. 2010.
- [32] S. Miura et al., "Scalability of quad interface p-MTJ for 1× nm STT-MRAM with 10-ns low power write operation, 10 years retention and endurance >10¹¹," IEEE Trans. Electron Devices, vol. 67, no. 12, pp. 5368–5373, Oct. 2020.
- [33] Z. Li and S. Zhang, "Thermally assisted magnetization reversal in the presence of a spin-transfer torque," *Phys. Rev. B, Condens. Matter*, vol. 69, no. 13, Apr. 2004, Art. no. 134416.
- [34] W. Rippard, R. Heindl, M. Pufall, S. Russek, and A. Kos, "Thermal relaxation rates of magnetic nanoparticles in the presence of magnetic fields and spin-transfer effects," *Phys. Rev. B, Condens. Matter*, vol. 84, no. 6, Aug. 2011, Art. no. 064439.